Design of Multiple-Stopband Filters for Interference Suppression in UWB Applications

K. Rambabu, Michael Yan-Wah Chia, *Member, IEEE*, Khee Meng Chan, and Jens Bornemann, *Fellow, IEEE*

***Abstract*—A design of multiple-stopband filters is presented for the suppression of interfering signals in UWB applications. Since possible interferers can be located at fixed frequencies or within a defined frequency band, the design of both fixed and tunable narrow stopband filter sections is addressed. For multiple fixed stopband filters, bent resonators, coupled to the main line, are introduced in order to more effectively suppress harmonics. A new tunable tapped stopband section is proposed, which allows the simultaneous control of stopband frequency and bandwidth. The final multiple-stopband design combines fixed and tunable sections and simultaneously suppresses interferences from global system for mobile communication, wireless local area network, worldwide interoperability for microwave access, and industrial–scientific–medical applications. Measurements verify the design process.**

***Index Terms*—Microstrip filters, multiband filters, stopband filters, ultra-wideband (UWB) applications.**

I. Introduction

ULTRA-WIDEBAND (UWB) technology started in 1960 as a time-domain study of electromagnetic wave propagation [1]. It finds applications in low-probability radar and in data communications. From a radar perspective, short-pulse UWB techniques have many advantages over conventional radar approaches [2]. In communication applications, short-pulse UWB techniques provide increased immunity to multipath cancellation and improve operational security. Moreover, low pulse-rate UWB technologies are ideally suited for battery-operated equipment. Due to the broad definition of UWB transmission technologies, various frequency bands are in use for different applications.

UWB radar for monitoring the motion of objects at short distance has been designed [3]. It operates between very low frequencies and 5 GHz and has also been applied to measure the heart and respiratory beats and other vital activities of patients. Through-wall UWB radars in the frequency range of 3.1–10.6 GHz are designed to detect people buried under debris [4].

UWB radar system designers have the option to utilize the wide frequency spectrum from very low frequencies up to 10.6 GHz. However, the power level allowed for UWB emitters in the frequency range of 1.61–10.6 GHz is lower than −41 dBm/MHz. Outside this band, emission should be reduced by another 10 dB. Measured interferences due to coexisting narrowband applications such as global system for mobile communication (GSM), wireless local area network (WLAN), worldwide interoperability for microwave access (WIMAX), and industrial–scientific–medical (ISM) are 20 dB stronger than the maximally permitted UWB emission. To operate UWB systems in the presence of such strong narrowband interferers is difficult at current power levels.

In this paper, we propose multiple-stopband filters to suppress narrowband interferences. Except for ISM band interference, which varies in frequency from 5 to 6 GHz with a bandwidth of 100 MHz, all other interferences are located at fixed frequencies. Therefore, Section II presents the design of narrow stopband filters with harmonic suppression. Section III introduces a tunable resonator with varying bandwidth for narrow stopband filters. In Section IV, both circuits are integrated into a multiple-stopband filter for UWB interference suppression.

Manuscript received December 25, 2005; revised April 20, 2006.

K. Rambabu, M. Y.-W. Chia, and K. M. Chan are with the Institute for Infocomm Research, Singapore 117674.

J. Bornemann is with the Department of Electrical and Computer Engineering, University of Victoria, Victoria, BC, Canada V8W 3P6.

Digital Object Identifier 10.1109/TMTT.2006.877813

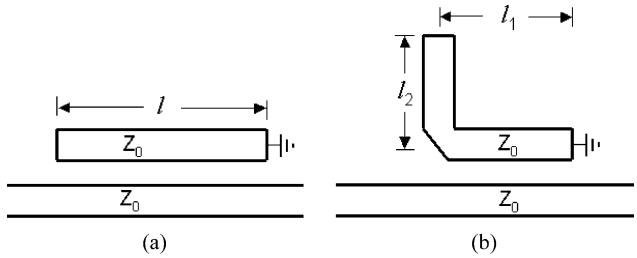

Fig. 1. Coupled resonator bandstop filter sections with: (a) straight and (b) bent resonators.

II. Fixed Stopband Sections

Different topologies are available for the design of fixed bandstop filters, e.g., open-circuit quarter-wavelength stubs, short-circuit half-wavelength stubs, and coupled resonators [5]. Generally, bandstop filters are concerned only with narrow frequency bands and bandwidths up to a few percent. Microwave stopband filters can be designed based on low-pass prototypes with suitable frequency transformation [6]. Coupled resonator bandstop filters are useful when relatively narrow stopbands are required. The resonator lengths are a quarter-wavelength at the center frequency of the stopband with a short circuit at one end. Resonators are capacitively coupled to the main line and spaced a quarter-wavelength apart at the stopband's center frequency [7]. In this paper, we use parallel-coupled resonator filters for suitable narrow stopbands.

Fig. 1 shows coupled resonator bandstop filter sections with straight and bent resonators. It is well known that maximum coupling occurs between coupled transmission lines, when the coupled line length is an odd multiple of a quarter-wavelength. If the coupled line length is an even multiple of a

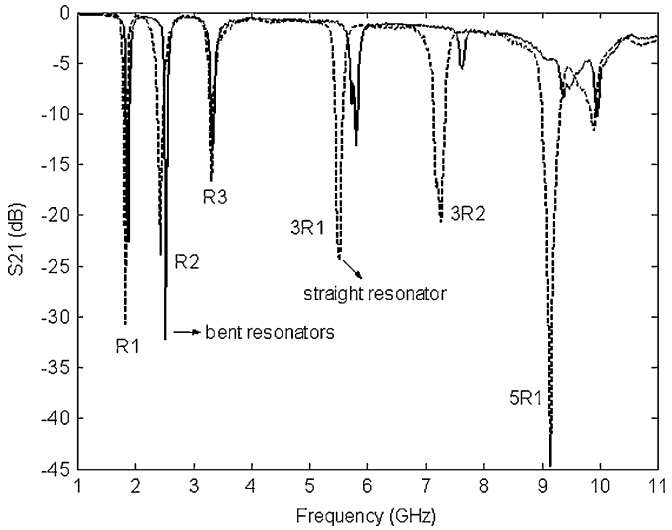

Fig. 2. Measured $|S_{21}|$ performances of five-stage multiple-stopband filter for GSM, WLAN, WIMAX, and ISM suppression using straight (dashed line) and bent resonators (solid line).

quarter-wavelength, then energy couples from the main arm to the coupled arm in the first quarter-wavelength section and back to the main arm in the following one. Therefore, even multiple quarter-wavelength coupling sections have minimum coupling.

In the configuration with straight resonators depicted in Fig. 1(a), the length l amounts to a quarter-wavelength including fringing fields and introduces stopbands at all odd harmonics. If a stopband at one of the harmonics needs to be suppressed, then the above concept is used in a bent configuration according to Fig. 1(b).

Within the prototype design presented in Section IV, let us consider that we want to eliminate the fifth harmonic of 1.84 GHz (9.2 GHz). A quarter-wavelength at 1.84 GHz results in the resonator length of $l_1 + l_2 = 24.5$ mm [see Fig. 1(b)] including fringing capacitances on a substrate material with $\varepsilon_r = 3.38$. To avoid the stopband at 9.2 GHz, this resonator is now bent such that the coupling section length $l_1 = 19.4$ mm (including fringing fields) is a full wavelength at 9.2 GHz.

Similarly, in order to eliminate the third harmonic of 2.44 GHz (7.32 GHz), the quarter-wavelength at 2.44 GHz is $l_1 + l_2 = 18.5$ mm on the same substrate (including fringing-field lengths). A half-wavelength at 7.32 GHz is $l_1 = 12.4$ mm [see Fig. 1(b)].

In order to effectively suppress GSM, WLAN, and WIMAX interference in UWB applications, the required attenuation levels are expected to be 20 dB (GSM and WLAN) and 15 dB (WIMAX). Since a single coupled-resonator stopband section will realistically produce an attenuation of approximately 16 dB, the sections to suppress GSM and WLAN have been doubled in the design presented in Section IV.

Here, in Fig. 2, we compare the measured results of a design using five straight resonators—two of them each doubled at two fundamental frequencies—with those of a similar design using bent resonators. According to the above examples, note that the harmonic stopbands labeled 5R1 (fifth harmonic of 1.84 GHz at 9.2 GHz) and 3R2 (third harmonic of 2.44 GHz at 7.32 GHz) are effectively suppressed using bent resonators (solid line).

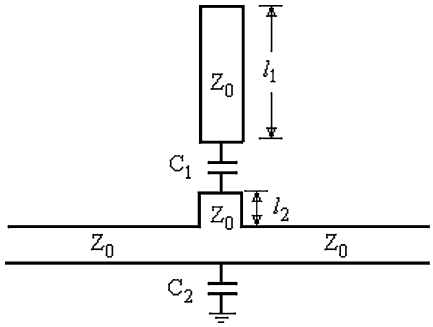

Fig. 3. Principal layout of the new tunable narrow bandstop section.

III. Tunable Stopband Section

Tunable bandpass or bandstop filters can be designed by loading the resonators (stubs) with variable capacitors. In general, for a stopband resonance to occur, an open-circuit quarter-wavelength resonator or a short-circuited half-wavelength resonator can be employed. The design of a narrow bandstop filter with conventional tunable stubs is difficult due to their low quality factor and the fact that maintaining a constant bandwidth over the entire range of frequencies is not possible.

In this paper, we propose a new tunable resonator (Fig. 3), which is different from conventional tapped resonators [8], [9] for the following reasons. First, the center frequency of the stopband can be tuned by tuning C_1, and the bandwidth can be controlled through C_2. Secondly, the resonator in Fig. 3 inherently possesses a high quality factor due to longer stub lengths required for its bandstop resonance. Thirdly, the bandwidth of this resonator is much narrower than that of the circuit in [9] due to the fact that the tuning capacitor is not located at the end of the stub. The resonator proposed here has an open-circuited stub (l_1), whose length is close to a half-wavelength, a capacitor C_1 and a very short stub (l_2). Although $l_1 + l_2$ are close to a half-wavelength, the total electrical length of the resonator (including C_1) is a quarter-wavelength at the center frequency of the stopband. Since the input impedance of an open-circuit quarter-wavelength resonator is zero, capacitor C_2 in parallel to the resonator will not affect the frequency of the stopband.

A. Theory

The resonance condition is obtained from the imaginary part of the input impedance

$$Z_0 \cot(\beta l_1) + \frac{1}{\omega C_1} - Z_0 \tan(\beta l_2) = 0. \tag{1}$$

For a given center frequency of the stopband, capacitance C_1 can be calculated as

$$C_1 = \frac{\tan(\beta l_1)}{Z_0 \omega (\tan(\beta l_1)\tan(\beta l_2) - 1)}. \tag{2}$$

The electrical length of the resonator decides the nature of the resonance. For a stopband, the phase should be

$$\beta l_2 + \cot^{-1}\left(\cot(\beta l_1) + \frac{1}{\omega C_1 Z_0}\right) = (2n-1)\frac{\pi}{2} \quad (3)$$

where n is an integer.

The total node admittance of the resonator including bandwidth-controlling capacitor C_2 can be written as (4), shown at the bottom of this page, and defines the quality factor of the resonator via

$$Q = \frac{\omega}{2G}\frac{\partial B}{\partial \omega}\bigg|_{\omega=\omega_0} \quad (5)$$

and, thus, (6), shown at the bottom of this page, where

$$P = \frac{C_1}{\sin(\omega K_1)\cos(\omega K_2)}\begin{bmatrix} \omega K_2 \dfrac{\cos(\omega K_1)}{\cos(\omega K_2)} \\ -\omega K_1 \dfrac{\sin(\omega K_2)}{\sin(\omega K_1)} \\ +\sin(\omega(K_1+K_2)) \end{bmatrix}$$

$$R = Y_0 K_2 \sec^2(\omega K_2)$$

$$S = \frac{-C_1}{\sin(\omega K_1)\cos(\omega K_2)}\begin{bmatrix} \omega K_1 \cos(\omega K_2)\sin(\omega K_1) \\ +\omega K_2 \sin(\omega K_1)\cos(\omega K_2) \\ -\cos(\omega(K_1+K_2)) \end{bmatrix}$$

$$K_1 = \frac{\sqrt{\varepsilon_{\text{reff}}}}{c} l_1$$

$$K_2 = \frac{\sqrt{\varepsilon_{\text{reff}}}}{c} l_2$$

and c is the speed of light. From (6), it follows that the quality factor of the circuit will increase with C_2.

B. Results

Fig. 4 shows the change in resonant frequency and bandwidth (-10 dB) of the resonator with tuning capacitor C_1 in the absence of C_2 and $l_1 = 14$ mm, $l_2 = 0.2$ mm. The solid line without diamonds or circles shows the capacitance calculated from (2) to change the resonant frequency from 4.8 to 6.2 GHz. The line with solid diamonds shows the capacitance variation calculated from ADS software and includes the junction effects and capacitor pad effects. The line with hollow diamonds is obtained from measuring the capacitance for different resonant frequencies. It is in good agreement with the capacitance from (2) over a wide frequency range. Of course, the bandwidth (line with circles) decreases with increasing resonant frequency due to less capacitive loading. For lower resonant frequencies and fixed l_1 and l_2, the required capacitive load is large compared to that required at higher resonant frequencies. Thus, the quality factor at lower resonant frequencies will be low.

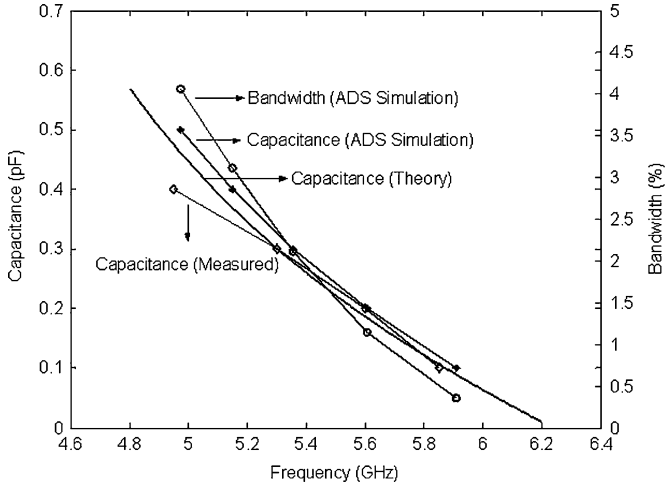

Fig. 4. Variation of center frequency and bandwidth with C_1 in the absence of C_2.

Fig. 5 displays the effect of C_2 on the resonant frequency and bandwidth for fixed quantities $C_1 = 0.1$ pF, $l_1 = 14$ mm, and $l_2 = 0.2$ mm. Equation (1) predicts no effect of C_2 on the resonant frequency, and (6) shows the increase in quality factor with C_2. Both facts are essentially confirmed by ADS simulations and measurements presented in Fig. 5. The differences between simulations and measurements are attributed to two facts: first, ADS is a circuit based, not a full-wave simulation tool and, second, the capacitance added by the solder material is not considered in the simulation.

It is possible to obtain a constant bandwidth throughout the tuning band by simultaneously adjusting C_1 and C_2. For $l_1 = 12$ mm and $l_2 = 0.2$ mm, Fig. 6 shows the required variation of C_1 and C_2 to achieve a constant -10-dB bandwidth of 4.5% while varying the center frequency from 5 to 6 GHz. C_1 is reduced to shift the resonant frequency from 5 to 6 GHz, and C_2 is reduced from 1.1 to 0.05 pF to maintain the constant bandwidth of 4.5% throughout the band.

$$Y_T = G + jB = 2Y_0 + j\left[Y_0\left(\frac{\omega C_1(1+\cot(\beta l_1)\tan(\beta l_2)) + Y_0\tan(\beta l_2)}{\omega C_1(\cot(\beta l_1) - \tan(\beta l_2)) + Y_0}\right) + \omega C_2\right] \quad (4)$$

$$Q = \frac{\omega}{4Y_0}\left[Y_0\left(\begin{array}{c} \dfrac{\{\omega C_1(\cot(\omega K_1) - \tan(\omega K_2)) + Y_0\}\{P+R\}}{\{\omega C_1(\cot(\omega K_1) - \tan(\omega K_2)) + Y_0\}^2} \\ -\dfrac{\{\omega C_1(1+\cot(\omega K_1)\tan(\omega K_2)) + Y_0\tan(\omega K_2)\}S}{\{\omega C_1(\cot(\omega K_1) - \tan(\omega K_2)) + Y_0\}^2} \end{array}\right) + C_2\right] \quad (6)$$

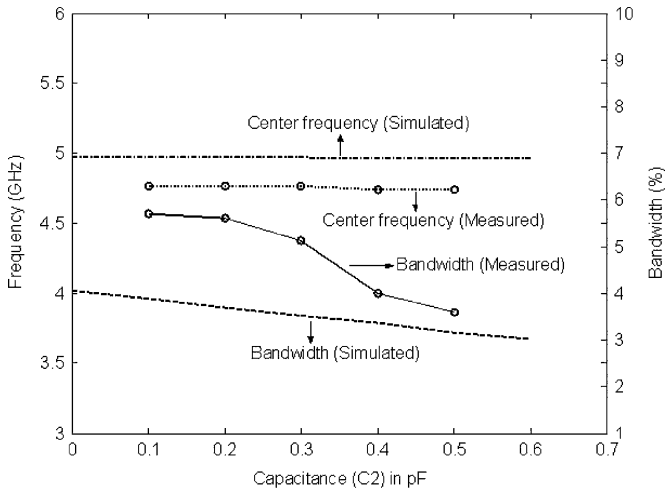

Fig. 5. Effect of C_2 on resonant frequency and bandwidth.

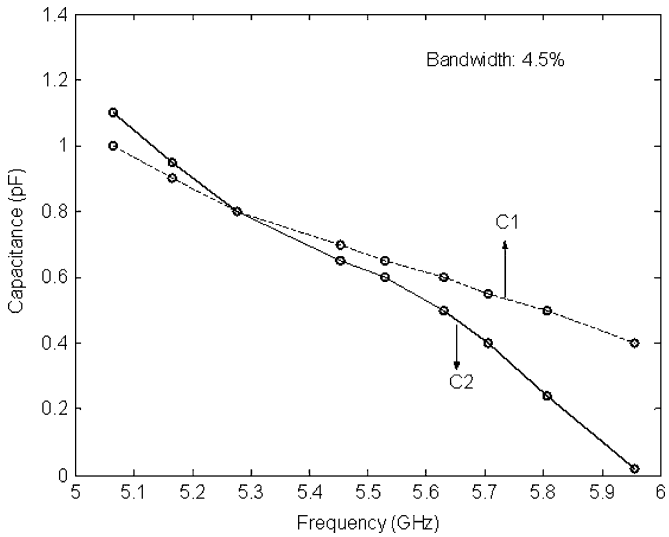

Fig. 6. Variation of C_1 and C_2 for constant bandwidth (ADS simulation).

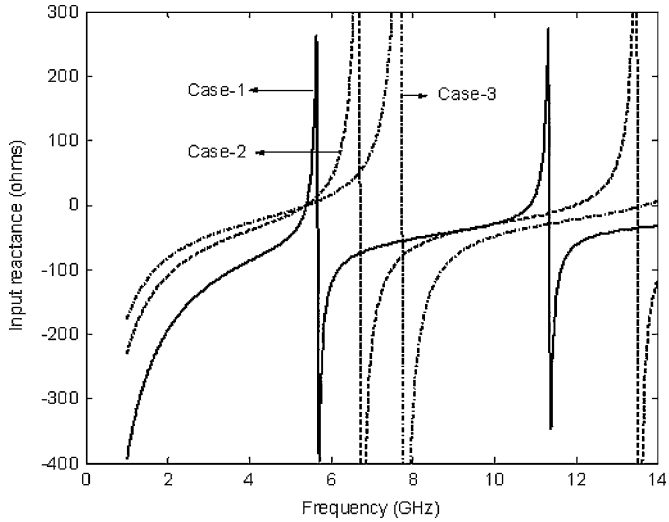

Fig. 7. Variation of reactance of input impedance for open-circuit resonator.

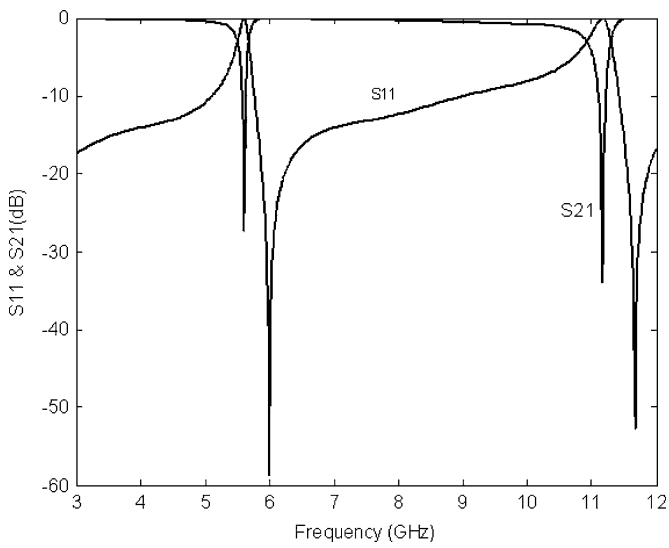

Fig. 8. Scattering parameters of tunable narrow bandstop section (case 1): simulated with ADS.

For practical microstrip lines, the impedance of an open circuit including fringing capacitances is in the order of a few hundred to a thousand ohms. The sequence of resonances (stopband and passband) can be estimated by calculating the imaginary part of the input impedance, as shown in Fig. 7. Stopbands and passbands occur at frequencies where the imaginary part of the input impedance vanishes.

For case 1, $l_1 = 15$ mm, $C_1 = 0.2$ pF, $l_2 = 0.2$ mm, and $C_2 = 0.2$ pF, the first stopband occurs at 5.4 GHz, the first passband at 5.75 GHz. The second stopband and passband are located at 10.87 and 11.35 GHz, respectively. This sequence is similar for case 2 ($l_1 = 12$ mm, $C_1 = 0.7$ pF, $l_2 = 0.2$ mm, $C_2 = 0.2$ pF) and case 3 ($l_1 = 10$ mm, $C_1 = 1.63$ pF, $l_2 = 0.2$ mm, $C_2 = 0.2$ pF). However, it can be seen from Fig. 7 that the harmonics of the stopband can be pushed upwards in frequency by reducing l_1 and increasing C_1. The ADS simulation in Fig. 8 (case 1 only) confirms the sequence of stopbands and passbands. It is an essential requirement for UWB applications that harmonic stopbands be pushed out of the frequency region where pulse energy is concentrated.

IV. Combined Fixed/Tunable Multiple-Stopband Filter

In full UWB band operation, harmonics of stopbands severely distort the pulse due to excessive loss at higher frequencies. Therefore, energy loss due to harmonics should be reduced to retain the pulse's shape.

In order to achieve a design for the fixed frequency stopbands for GSM, WLAN, WIMAX (Section II), and a variable stopband for ISM interference, the tunable tapped resonator section (Section III) is integrated with fixed coupled resonator filters sections presented in Section II. The final circuit is shown in Fig. 9. Note that compactness is achieved by structural folding and by varying the positions of individual resonators.

Following the microstrip line from the bottom left to top right, the bent resonator sections 1 and 3 as well as 2 and 5 are identical to satisfy the attenuation requirements in the GSM and WLAN bands (see Section II). They also suppress the undesired third harmonic of the WLAN and the fifth harmonic of

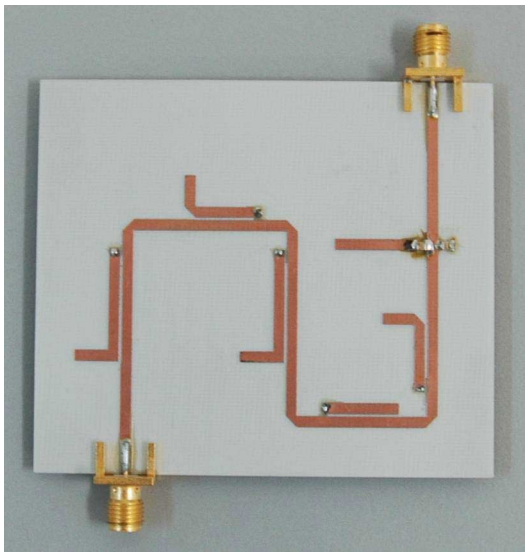

Fig. 9. Multiple-stopband filter for GSM, WLAN, WIMAX, and tunable ISM suppression. (Color version available online at: http://ieeexplore.ieee.org.)

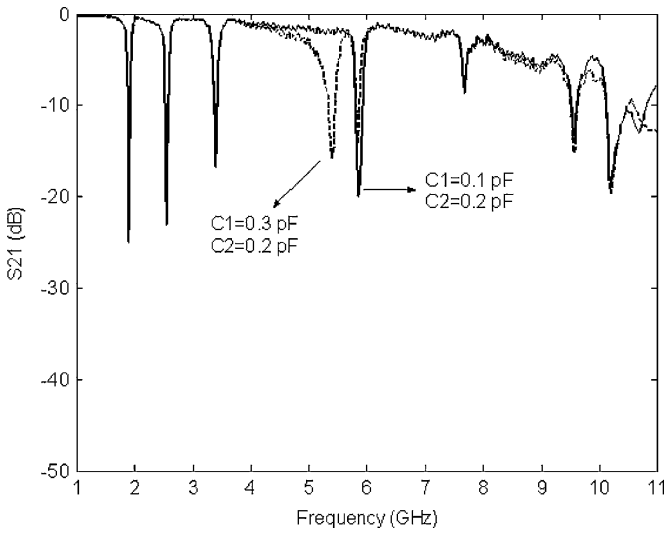

Fig. 10. Measured performances of the multiple-stopband filter for GSM, WLAN, WIMAX, and tunable ISM suppression.

GSM according to Section II. The main reason for not bending the small (fourth) resonator operating at 3.5 GHz (WIMAX) is that its harmonic is at 10.3 GHz, which is outside the frequency band of interest for UWB applications.

Fig. 10 displays the measured performances ($|S_{21}|$) of the integrated filter (Fig. 9) over the entire UWB frequency range and for two different sets of capacitances. It is obvious that this prototype circuit meets requirements encountered in UWB applications. Moreover, tunability over the ISM frequency range is demonstrated through two different sets of capacitances. However, it is also observed that the insertion loss increases markedly towards higher frequencies. Although losses at frequencies higher than 9 GHz will have only a small effect on UWB pulses due to the pulse's low energy content at those frequencies, the losses below 9 GHz are a concern. We attribute them as follows: first, losses of the microstrip lines increase with frequency; second, the prototype circuit is fabricated using simple means for circuit etching, the creation of the via-hole for C_2 and the placement and soldering of capacitors. Therefore, it is expected that utilizing suitable fabrication techniques can reduce insertion losses at higher frequencies.

V. Conclusion

The multiple-stopband printed-circuit filter scheme presented in this paper offers attractive solutions for the suppression of interferences in UWB applications. Bent resonators, which are coupled to the main line, allow the designer to control the stopband location and reduce the number of harmonics. Therefore, they are superior to hitherto known straight stopband resonators. The new tunable stopband section offers high design flexibility and presents a viable option to suppress interference from varying sources. The prototype design can be used to suppress interference from GSM, WLAN, and WIMAX applications, and additionally, allows tuning out signals in varying sections of the ISM band. Practical realization and prototype measurements validate the design process.

References

[1] C. L. Bennet and G. F. Ross, "Time-domain electromagnetics and its applications," *Proc. IEEE*, vol. 66, no. 3, pp. 299–318, Mar. 1978.

[2] R. J. Fontana, "Recent system applications of short-pulse ultra-wideband (UWB) technology," *IEEE Trans. Microw. Theory Tech.*, vol. 52, no. 9, pp. 2087–2104, Sep. 2004.

[3] I. Y. Immoreev, S. Samkov, and T. H. Tao, "Short-distance ultrawideband radars," *IEEE Aerosp. Electron. Syst. Mag.*, vol. 20, pp. 9–14, Jun. 2005.

[4] M. Y. W. Chia, S. W. Leong, C. K. Sim, and K. M. Chan, "Through-wall UWB radar operating within FCC's mask for sensing heart beat and breathing rate," in *Proc. 35th Eur. Microw. Conf.*, Paris, France, Oct. 2005, pp. 267–270.

[5] G. Matthaei, L. Young, and E. M. T. Jones, *Microwave Filters, Impedance Matching Networks, and Coupling Structures*. Boston, MA: Artech House, 1980, ch. 12.

[6] L. Young, G. L. Matthaei, and E. M. T. Jones, "Microwave bandstop filters with narrow stopbands," *IRE Trans. Microw. Theory Tech*, vol. MTT-10, no. 11, pp. 416–427, Nov. 1962.

[7] B. M. Schiffman and G. L. Matthaei, "Exact design of band-stop microwave filters," *IEEE Trans. Microw. Theory Tech.*, vol. MTT-12, no. 1, pp. 6–15, Jan. 1964.

[8] P. Rizzi, *Microwave Engineering-Passive Circuits*. Englewood Cliffs, NJ: Prentice-Hall, 1998.

[9] J. M. Drozd and T. Joines, "A capacitively loaded half-wavelength tapped-stub resonator," *IEEE Trans. Microw. Theory Tech.*, vol. 45, no. 7, pp. 1100–1104, Jul. 1997.

K. Rambabu received the Ph.D. degree from the University of Victoria, Victoria, BC, Canada, in 2004.

He is currently a Research Staff Member with the Institute for Infocomm Research, Singapore. He has authored or coauthored over 40 papers published in refereed journals and conferences. He holds a patent for beam shaping of a cellular base station antenna. His research interests include design and development of miniaturized passive microwave components and antennas for various applications.

Michael Yan-Wah Chia (M'94) was born in Singapore. He received the B.Sc. (first-class honors) and Ph.D. degrees from Loughborough University, U.K., in 1990 and 1994, respectively.

In 1994, he joined the Center for Wireless Communications (CWC), Singapore, as a Member of Technical Staff (MTS), and was then promoted to Senior MTS, then Principal MTS, and finally Senior Principal MTS. He is currently a Principal Scientist and Division Director with the Communications Division, Institute for Infocomm Research, A-STAR. He holds adjunct positions with the National University of Singapore and Nanyang Technological University of Singapore. In 1999, he started fundamental work on UWB research at I2R. Since then, his team has reported UWB transmission at a data rate of 500 Mb/s in April 2003 and 1 Gb/s in June 2004 conforming to FCC's mask. In 2002, he also led the development of a direct conversion transceiver design for wireless local area network (LAN) in collaboration with IBM. Since April 2004, his team has been invited into the IBM Business Partner Program for UWB-MBOA silicon design. He has authored or coauthored over 120 publications in international journals and conferences. He holds ten patents, some of which have been commercialized. His main research interests are UWB, beamsteering, wireless broadband, RF identification (RFID), antennas, transceivers, radio over fiber, RF integrated circuits (RFICs), amplifier linearization, and communication and radar system architecture.

Dr. Chia is a member of the Radio Standards (IDA), Telecommunications Standards Advisory Committee (IDA) and Technical Advisory Member of Rhode & Schwartz Communications & Measurements (Asia). He has been an active member of organizing committees in various international conferences and was program cochair of IWAT 2005. He was a keynote speaker at the International Conference of UWB in 2005. He is general chair of ICUWB 2007. He was the recipient of the Overseas Research Student Award and Studentship from British Aerospace, U.K.

Khee Meng Chan received the B.Eng. degree in electrical and electronic engineering from the University of Queensland, Brisbane, Qld., Australia, in 1997.

In 2001, he joined the Institute for Infocomm Research, Singapore, as a Research Engineer and was involved in projects developing RFID and UWB systems. He is currently a Senior Research Engineer with the Institute for Infocomm Research, where he is involved with passive and active circuits for a UWB radar project. His research interests are microwave filters, UWB systems, and circuit design.

Jens Bornemann (M'87–SM'90–F'02) received the Dipl.-Ing. and Dr.-Ing. degrees in electrical engineering from the University of Bremen, Bremen, Germany, in 1980 and 1984, respectively.

From 1984 to 1985, he was a Consulting Engineer. In 1985, he joined the University of Bremen, as an Assistant Professor. Since April 1988, he has been with the Department of Electrical and Computer Engineering, University of Victoria, Victoria, BC, Canada, where he became a Professor in 1992. From 1992 to 1995, he was a Fellow of the British Columbia Advanced Systems Institute. In 1996, he was a Visiting Scientist with Spar Aerospace Limited (now the MDA Corporation), Ste-Anne-de-Bellevue, QC, Canada, and a Visiting Professor with the Microwave Department, University of Ulm, Ulm, Germany. From 1997 to 2002, he was a Co-Director of the Center for Advanced Materials and Related Technology (CAMTEC), University of Victoria. In 2003, he was a Visiting Professor with the Laboratory for Electromagnetic Fields and Microwave Electronics, Eidgenössische Technische Hochschule (ETH) Zürich, Zürich, Switzerland. He coauthored *Waveguide Components for Antenna Feed Systems. Theory and Design* (Artech House, 1993) and has authored/coauthored over 200 technical papers. His research activities include RF/wireless/microwave/millimeter-wave components and systems design, and problems involving electromagnetic-field theory in integrated circuits, feed networks, and radiating structures. He serves on the Editorial Advisory Board of the *International Journal of Numerical Modeling*.

Dr. Bornemann is a Registered Professional Engineer in the Province of British Columbia, Canada. He serves on the Technical Program Committee of the IEEE Microwave Theory and Techniques Society (IEEE MTT-S) International Microwave Symposium (IMS).